THE AMERICAN MINERALOGIST, VOL. 51, MAY–JUNE, 1966

OPTICAL ABSORPTION SPECTRA OF IRON IN THE ROCK-FORMING SILICATES

WILLIAM B. WHITE AND KENNETH L. KEESTER, *Materials Research Laboratory and Department of Geochemistry and Mineralogy, The Pennsylvania State University, University Park, Pennsylvania.*

ABSTRACT

Optical absorption spectra have been obtained at 300° K. and at 78° K. on polished single crystals of low iron-content actinolite, olivine, diopside, epidote, chlorite and enstatite. The spectra cover the range of 400 to 3500 millimicrons. The single most characteristic feature is a strong band at 1000 millimicrons due to Fe^{2+} in six-fold coordination. This band varies in shape and intensity depending on the symmetry of the six-fold site. In diopside and enstatite a band occurs in the low frequency end of the spectrum which appears to be due to Fe^{2+} in four-fold coordination and suggests that a small amount of the ferrous iron is on the four-fold sites. Spectral bands assignable to ferric iron occur in the spectra of most minerals studied.

INTRODUCTION

That the green color of many common rock-forming silicates is due to the presence of ferrous iron has not been doubted since the earliest days of mineralogy. However, a detailed explanation for the color and its apparent change from one mineral to the next has not been forthcoming. The principal reason for this is an instrumental one. The green color of most iron-containing minerals is not due to an absorption band in the visible part of the spectrum but is rather due to a "window" in the visible between strong absorptions in the ultraviolet and the characteristic band of ferrous iron which occurs in the near-infrared. Only in perhaps the past five years have commerical instruments been available which operate routinely in the near-infrared. It seemed to be of value to investigate the spectra of the common silicates to see if useful structural information could be obtained from them. The study which we report is a preliminary reconnaissance in which six of the more common silicate structure types have been investigated.

Previous literature on this subject is sparse. Clark (1957) reported spectra of olivine, diopside and several garnets in the near-infrared region but he chose to interpret the spectra in terms of exiton bands rather than the more appropriate crystal field model. Application of the crystal field theory to geological problems has been attempted only recently by Curtis (1964) and Burns and Fyfe (1964). The use of the theory to interpret the spectra of iron-containing minerals has been carried out in considerable detail by Burns (1965a, b) in a study which came to our attention after our work was nearly complete. Burns used polarized radiation and oriented specimens so that his data are more detailed in the spectral range covered. However, the spectra in the present paper cover a wider wavelength range and are subjected to a somewhat different interpretation.

EXPERIMENTAL

We obtained specimens of clear single crystals of actinolite, olivine, diopside, epidote, chlorite and enstatite from commercial sources. The identities of the minerals were confirmed by optical and *x*-ray methods. Spectrographic analyses of all minerals were made to determine the iron and aluminum content and to check for the presence of other transition metal ions. A listing of the specimens is given in Table 1.

TABLE 1. SPECTROGRAPHIC ANALYSES[1] OF IRON-CONTAINING CRYSTAL SPECIMENS

Mineral	Locality	Fe_2O_3[2]	Al_2O_3	MnO	NiO	V_2O_5	Cr_2O_3	TiO_2
Actinolite	Gouveneur, New York	1.5	1.5	0.07	—	—	—	—
Olivine	Burma	8.5	0.15	0.14	0.40	—	—	—
Olivine	Kilbourne Hole, New Mexico	10	0.51	0.15	0.38	—	0.03	—
Diopside	Volonandrongo Tributary, Madagascar	2.0	2.4	0.06	—	—	—	0.06
Epidote	Salzburg, Austria	17	29	0.25	—	0.18	—	—
Enstatite	Burma	10	1.1	0.16	0.22	—	0.40	0.03
Chlorite	Corundum Hill, North Carolina	8.2	29	0.06	0.10	—	—	0.03

[1] All concentrations are in weight per cent.

[2] Includes both ferrous and ferric iron expressed as Fe_2O_3.

The minerals were cut into slices on the order of .5 to 3 mm thickness and polished. Where possible several crystallographic orientations were obtained. The slices were mounted on metal masks to limit the spectrophotometer beam to the polished area of the crystal. Spectra were obtained from 3500 to 400 millimicrons using a Beckman DK-2A spectrophotometer. Spectra at liquid nitrogen temperature were obtained with a special dewar flask of the type described by Lord *et al.* (1952) which fitted into the sample compartment of the spectrophotometer.

Diffuse reflectance spectra were obtained by packing powders into cupped holders similar to those commonly used for *x*-ray fluorescence analysis, and running these with an MgO-coated integrating sphere reflectance attachment. MgO was used as a reference material.

THEORY

The characteristic colors of transition metal ions both in aqueous solutions and in crystals are due to electronic transitions within the unfilled d-orbitals of the ions. The theoretical explanation for these effects in terms of the crystal or ligand field theory (Ballhausen, 1962; McClure, 1959) is now well established and can be applied directly to explanation of the iron mineral spectra.

This is not the place to attempt a review of crystal field theory and the reader is referred to the two reference books cited above. The d-electrons of transition metal ions are subjected to two sets of forces when the ions are incorporated in a crystal. First there is an interelectronic repulsion between the various electrons in the orbital. This interaction is described by the Racah B-parameter. The interelectronic repulsion causes a splitting of the d-energy level into a sequence of levels in the gaseous free ion. Secondly, the ion in a lattice site is subjected to an electrostatic field from the coordinating anions. This electrostatic interaction, the "crystal field," causes a further splitting of the free ion levels. The number and arrangement of crystal field energy levels is determined by the electronic symmetry of parent free-ion level and the geometrical site symmetry of the coordinating anions. The degree of splitting of the crystal field levels for each free-ion level is characterized by the crystal field splitting parameter, Dq. The observed electronic spectra of transition metal ions arise from transitions between the various crystal field levels, subject to certain selection rules.

Since there are two competing forces on the d-electrons there exists the possibility for either the interelectronic repulsion or the crystal field to be the dominant force. Respectively, these are the weak field and the strong field cases. In the weak field case, the ground state has the same electronic symmetry and spin multiplicity as the free ion while at the strong field boundary there is a cross-over of levels and a different level becomes the ground state usually accompanied by a change in spin multiplicity which results in different selection rules and thus a totally different spectrum. A weak field usually implies tightly bound d-electrons with relatively little interaction with the coordinating anions while strong fields imply a high degree of interaction and thus covalent bonding. Ions of low charge coordinated by oxide anions are usually described by the weak field diagram. The energy level schemes described above can be computed in a general way for each d-electron configuration in terms of B and Dq. The calculated levels for octahedral coordination are known as Tanabe-Sugano diagrams (Tanabe and Sugano, 1954) and have been widely reprinted, being given in both general references cited above and in many other review articles.

From a structural interpretation point of view, an important factor in crystal field spectra is that one can make rigorous interpretations based on theory without the necessity of empirical correlations, necessary in the case of vibrational spectra for example. The spectrum arising from a given transition metal ion is influenced by the following parameters in order of importance:

i. The coordination number and valence state: by far the most important factors; these determine the main features of the spectra.
ii. The nature of the ligand: since this study concerns only oxygen coordination, this factor is fixed.
iii. The distortion of the transition metal ion site: distortions from pure octahedral or tetrahedral coordination may cause splitting of the bands.
iv. Metal-oxygen distances: a relatively small effect.

Because of the dominant influence of the first factor, one can make reliable assignments of observed spectra of the silicates by direct comparison with the spectra of the same ion in simpler oxide structures where the coordination is known. One can also predict the spectra from the known energy level diagrams.

The spectra of iron-containing silicates involve only the energy level schemes of ferrous and ferric iron. These schemes can be taken directly from the more general Tanabe-Sugano diagrams which give the correct labeling for the levels and an estimate of their positions. The diagrams for Fe^{2+} and Fe^{3+}, based on the values of Dq and B given in Table 2, are shown in Figs. 1 and 2. The ground state of ferrous iron is a D state which splits in an octahedral crystal field into an upper quintet Eg level and a lower quintet T_{2g} level separated by about 9000 cm^{-1}. No other quintet states are present so there is only one spin-allowed transition which should give rise to a single absorption band at about 9000 cm^{-1} or 1100 millimicrons in the near-infrared. There are additional levels between 16,000 and 30,000 cm^{-1} but transitions from the ground state to these levels are spin-forbidden and the resulting spectra are expected to be very weak. The predicted spectrum, therefore, for ferrous iron substituting for magnesium in the six-fold sites in a silicate, is a single intense band at 1100 millimicrons, and possibly a few weak bands below 630 millimicrons.

Ferric iron has a d^5 electron configuration and, therefore, a symmetric S ground state. ^6S does not split in any crystal field and is the only sextet state present. Transitions to the higher levels arising from the ^4G state are all spin forbidden and any bands present would be expected to be weak.

The spectra of Fe^{2+} has been determined in a number of hosts and some measurements have been made on Fe^{3+} although its spectrum is more poorly known. Data for the main allowed transition of Fe^{2+}, the several

TABLE 2. BAND POSITIONS AND CRYSTAL FIELD PARAMETERS FOR IRON IONS IN VARIOUS OXIDE HOSTS

Octahedral Fe^{2+}

$B=917\ cm^{-1}$

$^5T_{1g}\rightarrow{}^5E_g$	Dq	Host	Reference
10,400 cm^{-1}	1040 cm^{-1}	$Fe(H_2O)_6^{2+}$	Holmes and McClure (1957)
10,000	1000	MgO	Low and Weger (1960)
9,100	910	Soda-lime-silica glasses	Bates (1962)

Tetrahedral Fe^{2+}

$B=917\ cm^{-1}$

$^5E\rightarrow{}^5T_1$	Dq	Host	Reference
4,500	450	ZnO	Bates, White and Roy (1966)
4,300	430	$MgAl_2O_4$	Slack (1964)

Octahedral Fe^{3+}

Observed Transitions		B[1]	Dq	Host	Reference
$^6A_{1g}\rightarrow{}^4T_{1g}$	14,200	700		Beryl	Dvir and Low (1960)
$\rightarrow{}^4T_{2g}$	17,500				
	20,000				
$\rightarrow{}^4Eg,\ {}^4A_{1g}$	23,600				
$^6A_{1g}\rightarrow{}^4T_{2g}$	18,200	760	1650	Corundum	McClure (1962)
$\rightarrow{}^4E_g,\ {}^4A_{1g}$	25,600				
$^6A_{1g}\rightarrow{}^4T_{1g}$	12,600	730	1400	$[Fe(H_2O)_6^{3+}]$	Holmes and McClure (1957)
$\rightarrow{}^4T_{2g}$	17,200				
$\rightarrow{}^4Eg,\ {}^4A_{1g}$	24,500				

[1] Calculated from $^6A_{1g}\rightarrow(^4Eg,\ {}^4A_{1g})$ transition by means of the Tanabe-Sugano matrices. $\Delta E=10B+5C$. C/B assumed to be 4.73 (McClure 1959).

lower levels of Fe^{3+} and the derived crystal field parameters are given in Table 2.

SINGLE CRYSTAL SPECTRA AND ASSIGNMENTS

Spectrum of actinolite. Of the minerals studied the simplest spectrum is that of actinolite which is shown in Fig. 3. The section observed is a 110 cleavage face. The spectrum in Fig. 3 was taken at liquid nitrogen temperature but the room temperature spectrum is very similar. In general cooling to 78° K. has very little effect on the silicate spectra, contrary to expectations.

The single electronic transition in actinolite occurs at 9800 cm^{-1} and

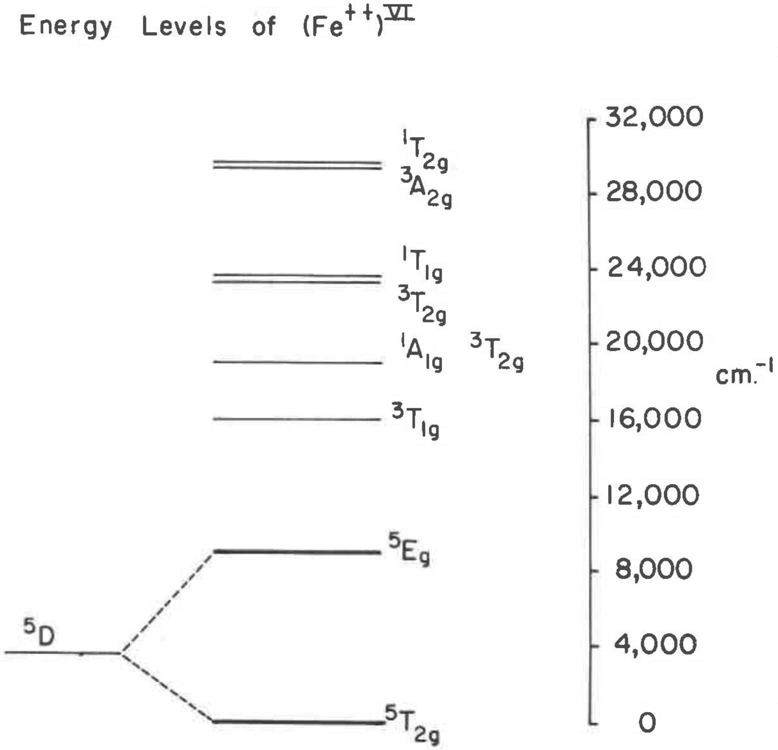

FIG. 1. Energy level scheme for ferrous iron in octahedral coordination. Sketched from Tanabe-Sugano diagrams using an estimate value of $Dq/B=0.9$. Free-ion levels given on left.

is easily identified as the $T_{2g}\rightarrow Eg$ band of ferrous iron in six-fold coordination. The spectrographic analysis of this specimen shows 1.5 per cent iron with .07 per cent manganese and no other transition element identified. The symmetry and sharpness of the band is also understandable from the structure determination by Zussman (1955) in which he shows that the metal-oxygen distances in actinolite are on the order of 2.11 angstroms. In actinolite, the oxygen coordination octahedron is only slightly distorted and only a single band appears in the optical spectrum.

In addition to the electronic band due to d-d transitions, all of the silicate spectra contain a number of very sharp bands due to vibrational spectra of the hydroxyl ion. Actinolite exhibits these particularly well because of its essential OH^- group but all other silicates including olivine have some impurity OH^- which gives rise to near-infrared absorption. In the spectrum of actinolite in Fig. 3, the strong band at 2320 millimicrons is a combination band; the OH^- fundamental stretching frequency is beyond the end of the spectrum at 2750 millimicrons. The very sharp band at 1400 millimicrons is the seond harmonic of the OH^- stretching mode. Much detailed interpretation and some crystallographic information can be obtained from the OH^- bands. This will be the subject of a separate paper.

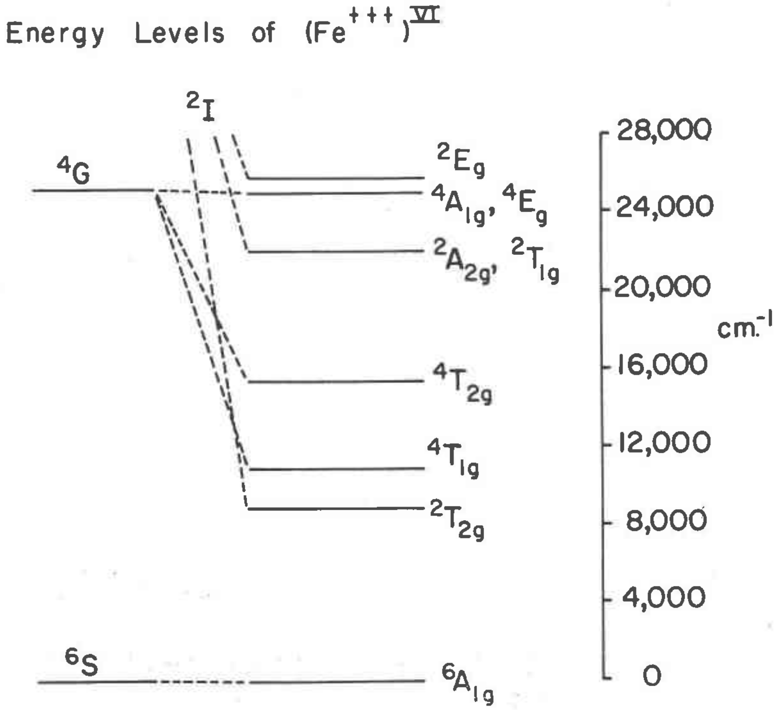

FIG. 2. Energy level scheme for ferric iron in octahedral coordination. Sketched from the Tanabe-Sugano diagrams with an estimated value of $Dq/B = 2.17$ based on McClure's (1962) data for Fe^{3+} in corundum. The free-ion levels are shown on the left.

As will be discussed later, the position of the hydroxyl ion absorptions overlaps the absorption due to tetrahedral ferrous iron. Vibrational and electronic spectra can best be separated by their bandwidths. The vibrational bands are much narrower. However, the abcissae of the spectra are not linear in energy so a comparison cannot be made directly between bands in different regions of the spectrum. In the actinolite spectrum of Fig. 3, the half width of the $(Fe^{2+})^{VI}$ band is 1360 cm^{-1} while the 2320 millimicron and 2390 millimicron hydroxyl bands have half widths of 65 and 40 cm^{-1}.

Spectrum of olivine. The next more complicated iron silicate spectrum is that of olivine shown in Fig. 4. Again the absorption band due to ferrous iron is clearly visible. The effect of cooling the specimen to liquid nitrogen temperature is to shift the major peak by 170 cm^{-1}, a minor shift to higher energy easily accounted for by the decrease in metal oxygen distances due to thermal contraction of the structure. In olivine, the ferrous iron band is not symmetrical and has shoulders on both high and low frequency sides. These arise from the rather wide distribution of metal oxygen distances ranging from 2.06 angstroms to 2.22 angstroms which lower the site symmetry of the Fe^{2+} ion. According to the point charge model, the crystal field splitting parameter and, therefore, the energy of the band varies with the fifth power of the interatomic distances and thus changes in the metal oxygen distance cause measurable shifts in

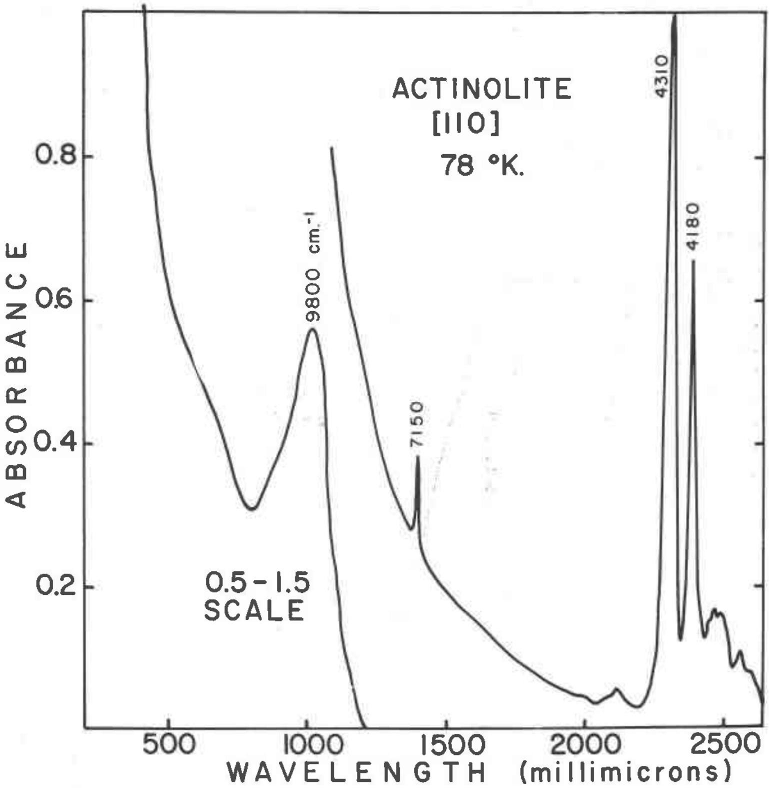

FIG. 3. Optical spectrum of single crystal actinolite. {110} cleavage face 78° K. Thickness = 2.27 mm.

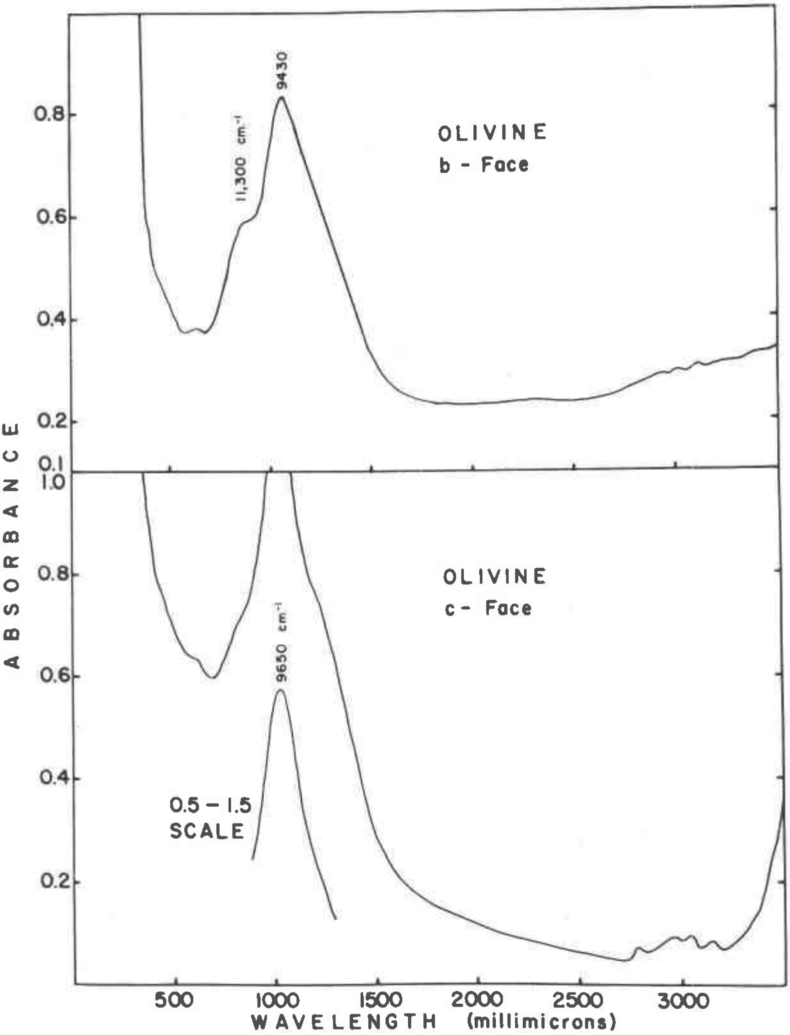

FIG. 4. Optical spectrum of single crystals of olivine. 300° K. Thickness: b-face = 0.83 mm, c-face = 0.71 mm.

the peak position. Burns (1965a) discusses the splitting of the $(Fe^{2+})^{VI}$ band of olivine in more detail.

The weak band at 15,900 cm^{-1} (630 mμ) appears to be due to a trace of ferrous iron. It corresponds almost exactly to the predicted position of the $^6A_{1g} \rightarrow {}^4T_{2g}$ transition shown in Fig. 2.

Spectrum of diopside. The spectrum of diopside is shown in Fig. 5. The features here become considerably more complicated. In the region of iron absorption are three bands, a weaker one at 13,600 cm^{-1}, a very intense band at 9730 cm^{-1} and a broad band at 4420 cm^{-1}. The spectrographic analyses show two per cent iron with traces of only manganese and titanium so that the entire spectrum must be explained in terms of iron, although possibly in terms of iron in two valence states. The intense band at 9730 cm^{-1} is quite clearly due to ferrous iron in six-fold coordination as it is in essentially the same position as the band of minerals previously discussed.

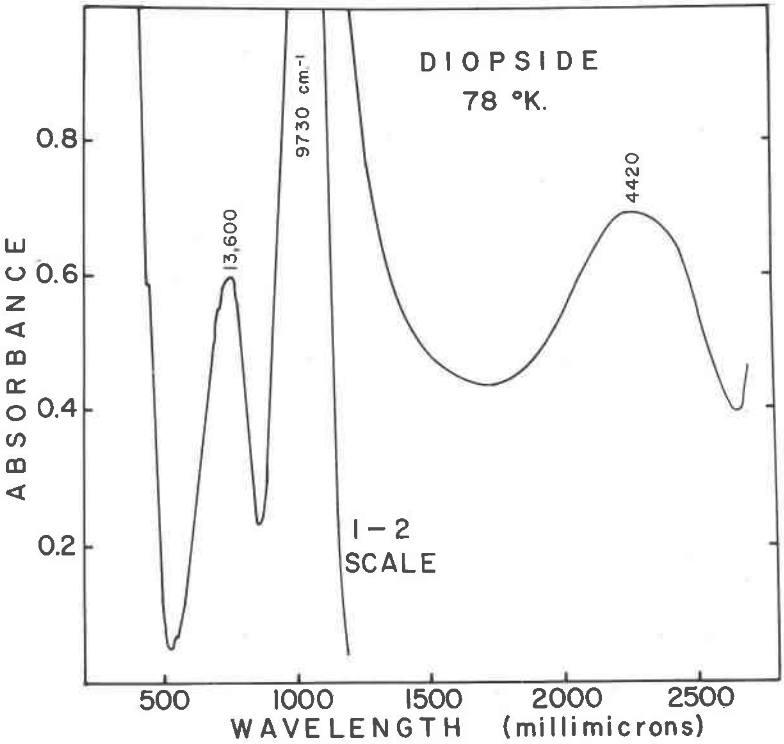

FIG. 5. Optical spectrum of single crystal diopside. 78° K. Average thickness = 4.14 mm.

There are three possibilities for the high energy band. The first is that the high energy band is due to a spin-forbidden transition in ferric iron and indeed there is reasonable agreement between the position of the band and the first transition of Fe^{3+} in beryl (Table 2). The second possibility is that the two high energy bands both arise from Fe^{2+} in the six-fold sites since the levels may be split because of the lower site symmetry. Although the octahedra in diopside are distorted, it does not seem likely that the distortions would cause a splitting of 3900 cm^{-1}. The third possibility is that ferrous iron has substituted for calcium on the eight-fold site. This possibility, however, is in disagreement with the spectrum. The crystal field splitting parameter for eight-fold coordination is only $\frac{8}{9}$ of the value of six-fold coordination. Also the calcium-oxygen distances are larger than the magnesium-oxygen distances. Both of these factors would tend to lower rather than raise the energy and thus any eight-fold band should occur on the low frequency side of the $(Fe^{2+})^{VI}$ band. Therefore, it is most likely that the band arises from ferric iron.

The broad band at 4420 cm^{-1} is of most interest. It is almost certainly due to ferrous iron in four-fold coordination. Two arguments support this conclusion. Firstly, in the point charge approximation, Dq for tetrahedral coordination is expected to be $\frac{4}{9}$ of its value for octahedral coordination if the interatomic distances do not change. Taking four-ninths of the energy of the octahedral iron band yields 4330 cm^{-1} in reasonable agreement with the observed value of 4420 cm^{-1}. Secondly, the observed band position agrees well with the reflectance spectrum of ferrous iron-doped zinc oxide in which the iron also occurs in tetrahedral coordination (Table 2). Thus, we conclude that in diopside, a small percentage of the iron occurs in the tetrahedral sites. This is in agreement with results recently obtained by Colville and Gibbs (1964) in which they find tetrahedral iron in riebeckite.

It should be made quite clear that the amount of ferrous iron present on the silicon sites is very small. The total iron present in this diopside crystal is only two per cent. The bulk of this is present as Fe^{2+} on the octahedral sites as the intense band at 9730 cm^{-1} indicates. In addition, the absolute intensities of tetrahedral ion transitions are from 10 to 100 times larger than corresponding octahedral transitions. Thus, the amount of ferrous iron on the tetrahedral sites is probably less than 0.1%.

Spectrum of epidote. The spectrum of epidote is shown in Fig. 6. The interpretation of the spectrum is largely a repetition of what has gone before. The octahedral ferrous iron band occurs as expected although it is much weaker suggesting that relatively little of the iron is in the ferrous state. The relatively strong band at 16,500 cm^{-1} is again assigned to ferric iron. Because of the nature of the energy level diagram for ferric iron and because only the lowest transition is obtained, it is not possible to determine the coordination number of the ion. Attention should be called to the broad absorption feature at 3380 cm^{-1}. This again has the appearance, although obscured by the sharp peaks due to hydroxyl ion, of being due to ferrous iron in tetrahedral coordination. However, the low energy of the band makes this assignment uncertain, and, if the assignment is correct, the site must be one with unusually large metal oxygen distances.

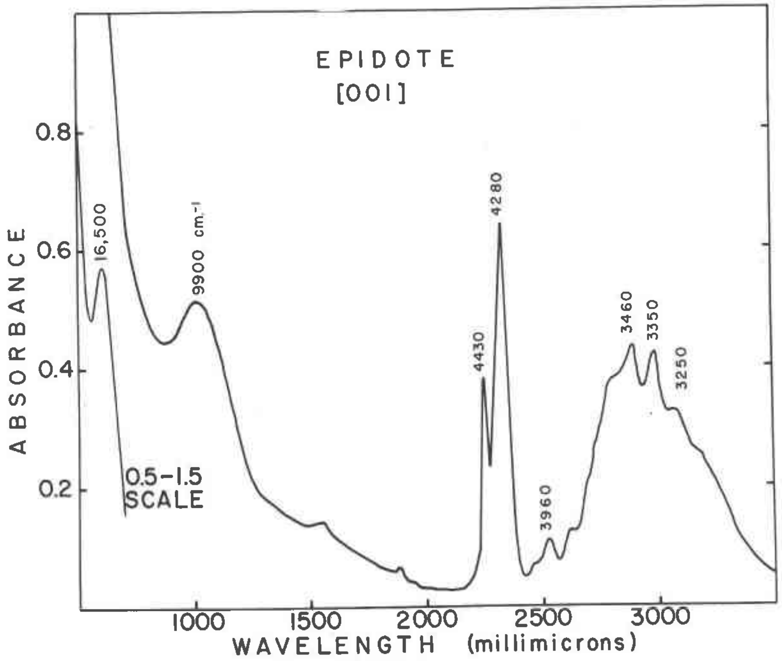

FIG. 6. Optical spectrum of single crystal epidote. {001} face. 300° K. Thickness = 1.04 mm.

Spectrum of chlorite. The spectrum of chlorite is shown in Fig. 7. This spectrum is distinctly different from the others thus far presented in that it is dominated by ferric rather than ferrous iron. The band due to octahedral Fe^{2+} appears only as a weak shoulder. There is no evidence for tetrahedral Fe^{2+} although the characteristic region of the spectrum is obscured by intense hydroxyl absorption. There are more differences between the room temperature and liquid nitrogen temperature spectra of chlorite than for any other silicate studied. For this reason both spectra are included in Fig. 7. The differences take the form of small frequency shifts and large changes in intensity.

The frequencies and assignments of the bands in Fig. 7 are tabulated in Table 3. Chlorite provides one of the most distinct spectra of Fe^{3+} yet reported. It should be noted that the "window" in the spectrum at 525 $m\mu$ is between two ferric iron bands and thus the green color of chlorite is due to ferric iron.

The 24,700 cm^{-1} band of chlorite is assigned to the transition between the $^6A_{1g}$ ground state and the ($^4A_{1g}$, ^4E_g) level. This particular transition is independent of the crystal field strength and the Racah B-parameter can be calculated directly by means of the Tanabe-Sugano matrices.

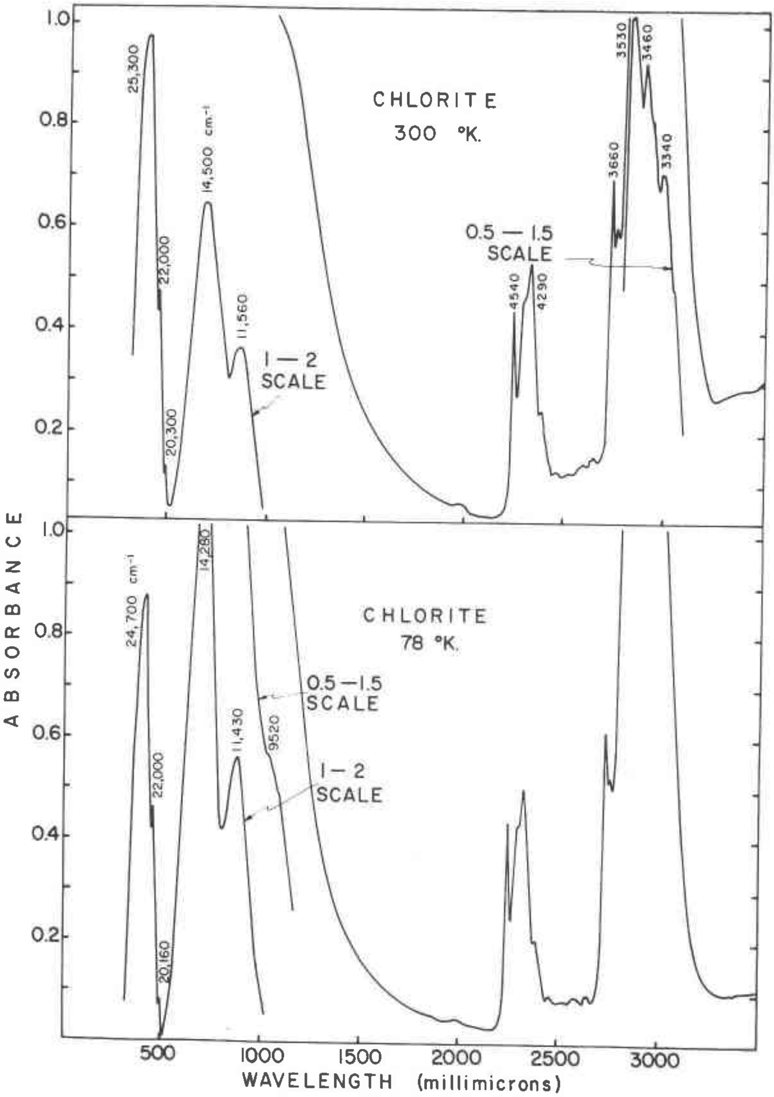

FIG. 7. Optical spectrum of single crystal chlorite. {001} basal cleavage section. Both 78° K. and 300° K. spectra shown. Thickness = 0.27 mm.

The Racah B-parameter of Fe^{3+} in chlorite is found to be 734 cm^{-1}, a value very similar to those listed in Table 2 for Fe^{3+} in other host lattices. The crystal field splitting parameter, Dq, can be calculated exactly only solving high order Tanabe-Sugano matrices which the precision of the present data does not warrent. However, an approximate value can be found by

TABLE 3. ELECTRONIC ABSORPTION BANDS OF IRON IN CHLORITE BASED ON 78° K. SPECTRUM (FIG. 7)

Wavelength mμ	Wave Number cm^{-1}	Description	Assignment	
1050	9,520	Shoulder	$(Fe^{2+})^{VI}$	$^5T_{2g} \rightarrow {}^5Eg$
875	11,430	Med. Band	$(Fe^{3+})^{VI}$	$^6A_{1g} \rightarrow {}^4T_{1g}$
700	14,280	Strong Band	$(Fe^{3+})^{VI}$	$^6A_{1g} \rightarrow {}^4T_{2g}$
496	20,160	Weak, very sharp	$(Fe^{3+})^{VI}$	$^6A_{1g} \rightarrow A_{2g}$, $^2T_{1g}$
454	22,000	Weak, very sharp		
405	24,700	Strong Band	$(Fe^{3+})^{VI}$	$^6A_{1g} \rightarrow (^4A_{1g}, {}^4Eg)$

matching the observed spectrum against the Tanabe-Sugano energy level diagram. This procedure yields a Dq of 1600 cm^{-1} indicating that the crystal field of chlorite is very similar to that of corundum.

Spectrum of enstatite. The spectrum of enstatite shown in Fig. 8 is quite remarkable. There is a profusion of bands whose wavelengths are tabulated in Table 4. The spectrographic analysis does very little to clarify the situation. The iron content is 10% with only .22% nickel and .40% chromium.

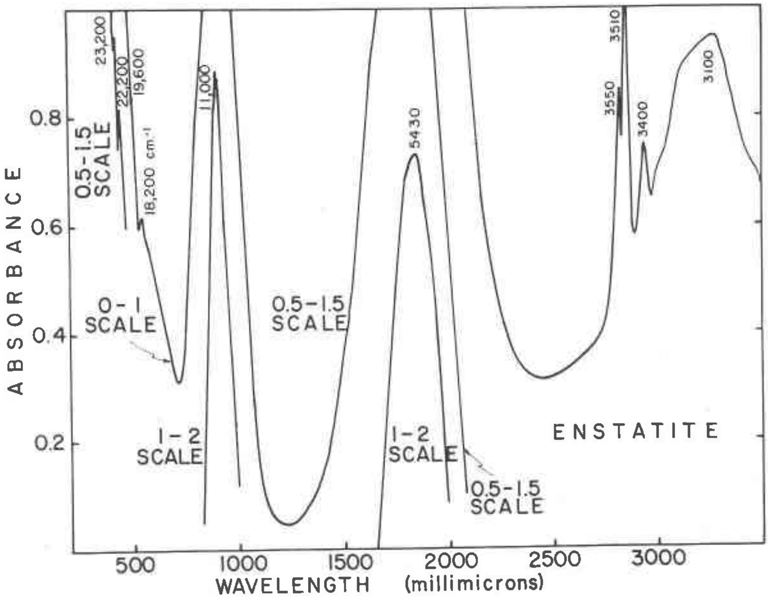

FIG. 8. Optical spectrum of single crystal enstatite. 300° K. Thickness = 1.34 mm.

The strong band at 11,000 cm^{-1} is probably the characteristic band of Fe^{2+} in six-fold coordination although it is shifted to somewhat higher energies than the $(Fe^{2+})^{VI}$ band in the other silicates. The assignment of the two low frequency bands poses a number of problems. Both are in the spectral range where absorption from $(Fe^{2+})^{IV}$ is expected to occur. It seems most reasonable to assign the 5430 band to Fe^{2+} on the silicon sites although the energy is 25% higher than the $(Fe^{2+})^{IV}$ band in diopside and the other oxide hosts listed in Table 2. The other low frequency band at 3220 cm^{-1} appears to be an overtone of the vibration of the silicate framework. In spectra obtained at longer wavelengths, the band forms part of a continuous absorption extending into the vibrational region. The weak sharp bands arise from spin-forbidden transitions in Fe^{2+}. Tentative assignments are listed in Table 4.

TABLE 4. BAND POSITION IN ENSTATITE

Wavelength (m*u*)	Frequency (cm^{-1})	Description	Assignment	
3220	3,100	Med. Broad	Vibrational overtone	
1840	5,430	Strong, Broad	$(Fe^{2+})^{IV}$	$^5E \rightarrow {}^5T_2$
910	11,000	Strong, Broad	$(Fe^{2+})^{VI}$	$^5T_{2g} \rightarrow {}^5Eg$
550	18,200	Weak, Sharp	$(Fe^{2+})^{VI}$	$^5T_{2g} \rightarrow {}^3T_{1g}$
510	19,600	Very Weak, Sharp	$(Fe^{2+})^{VI}$	$^5T_{2g} \rightarrow {}^1A_{1g}$(?)
450	22,200	Weak, Sharp	$(Fe^{2+})^{VI}$	$^5T_{2g} \rightarrow {}^3T_{2g}$
431	23,200	Weak, Sharp	$(Fe^{2+})^{VI}$	$^5T_{2g} \rightarrow {}^1T_{1g}$(?)

The Tanabe-Sugano matrices for the quintet levels of ferrous iron are such that the spin-allowed transition is independent of B. Although Dq can be obtained by simply dividing the transition energy by 10, B can be estimated only by matching the weak spin-forbidden transitions with the Tanabe-Sugano diagram. Unfortunately the Tanabe-Sugano diagram for the d^6 case is not complete. Although tentative assignments for the weak bands are listed in Table 4, other triplet free ion states occur whose behavior under a crystal field has not been calculated. In view of these uncertainties, a value for B has not been estimated.

DIFFUSE REFLECTANCE SPECTRA

Diffuse reflectance spectra were obtained from finely-ground powders of all specimens except chlorite. The spectra are shown in Fig. 9. Of most importance is the fact that the electronic features observable in the single crystal spectra also appear in the reflectance spectra although with reduced intensity. The vibrational transitions due to OH^- are almost

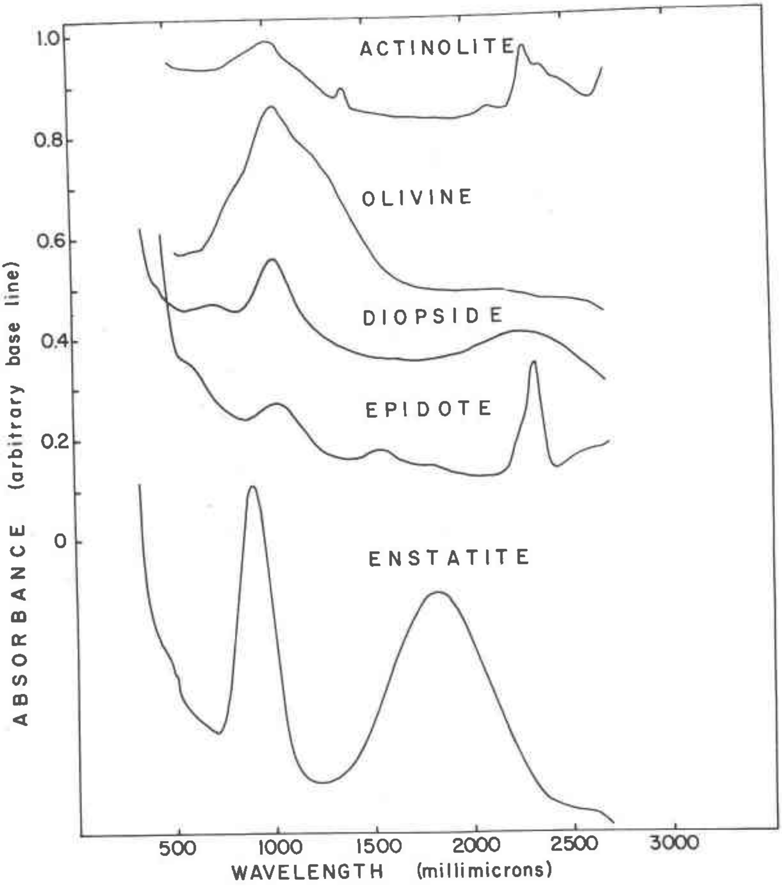

FIG. 9. Diffuse reflectance spectra of iron-containing silicate minerals at 300° K.

completely eliminated. It is, therefore, possible to conduct studies of the behavior of iron in silicates using powdered specimens.

DISCUSSION AND CONCLUSIONS

Origin of the Spectra of Iron-Containing Minerals. An explanation for the visible and near-infrared absorption spectra of the iron-containing silicate minerals is of significance in its own right. This has been done in preceding sections in terms of crystal field theory. It should be emphasized that most of the assignments, and particularly the ferrous iron bands, are quite rigorous due to the insensitivity of the energy levels to other than the first sphere of coordination.

Tetrahedral Iron. In enstatite and diopside, the low energy band has been interpreted as arising from Fe^{2+} in four-fold coordination. Two points must be made concerning tetrahedral iron. The first is that the assignment is moderately rigorous. Fe^{3+} has no absorption in this region in either four- or six-coordination. The frequency of the tetrahedral band is close to four-ninths of the frequency of the octahedral band as required by the point charge model of the crystal field theory. The agreement with the observed spectra of Fe^{2+} in the tetrahedral sites in ZnO and $MgAl_2O_4$ is good. The second point is that although Fe^{2+} seems to be definitely present on the tetrahedral sites, the amount is very small. The molar extinction coefficients of tetrahedral bands in general are *ca.* 100 times larger than the extinction coefficients of the corresponding octahedral bands. In enstatite the two bands are of comparable intensity so of the 10% iron present in the specimen no more than 0.1% is likely on the tetrahedral sites. In diopside the amount must be still smaller.

The particular importance of these results is that (i) Fe^{2+} does indeed substitute for silicon as some *x*-ray studies have indicated, and (ii) that the optical spectrum makes a particularly sensitive tool for studying this phenomenon. For example, one may now write the formula for diopside as:

$$[\mathrm{Ca}^{2+}]^{\mathrm{VIII}}[\mathrm{Mg}_{1-\mathrm{x}}\mathrm{Fe}^{2+}_{\mathrm{x}-3\mathrm{y}}\mathrm{Fe}^{3+}_{2\mathrm{y}}]^{\mathrm{VI}}[\mathrm{Si}_{2-\mathrm{y}}\mathrm{Fe}^{2+}_{\mathrm{y}}]^{\mathrm{IV}}\mathrm{O}_6$$

where x is the amount of iron in the crystal and y (much less than x) is the amount of tetrahedral substitution. From this formula, it can be seen that the tetrahedral substitution of ferrous iron is part of the charge compensation that must occur with the oxidation of small amounts of iron to the trivalent state. Substitution of Fe^{3+} on the tetrahedral sites probably also takes place but the spectra do not give a sensitive measure of this effect.

ACKNOWLEDGEMENTS

This work was supported by the National Science Foundation under Grant Number GP-3232.

REFERENCES

BALLHAUSEN, CARL J. (1962) *Introduction to Ligand Field Theory.* McGraw-Hill Book Co., New York.

BATES, CARL, WILLIAM B. WHITE AND RUSTUM ROY (1966) The solubility of transition metal oxides in zinc oxide and the reflectance spectra of Mn^{++} and Fe^{++} in tetrahedral fields, *Jour. Inorg. Nucl. Chem.* **28,** 397–405.

BATES, T. (1962) Ligand field theory and absorption spectra of transition-metal ions in glasses. In, *Modern Aspects of the Vitreous State,* Butterworths, London, 195–254.

BURNS, ROGER G. (1965a) Electronic spectra of silicate minerals: application of crystal field theory to aspects of geochemistry. Ph.D. Diss., Univ. California, Berkeley.

——— (1965b) Origin of pleochroism in "hypersthenes." Paper presented, *Ann. Meet. M.S.A.*, Gatlinburg, Tennessee.

——— AND WILLIAM S. FYFE (1964) Site of preference energy and selective uptake of transition-metal ions from a magma. *Science* **144,** 1001–1003.

CLARK, SYDNEY P., JR. (1957) Absorption spectra of some silicates in the near infrared *Am. Mineral.* **42,** 732–742.

COLVILLE, ALAN A. AND GERALD V. GIBBS (1964) Refinement of the crystal structure of riebeckite. *Geol. Soc. Am. Spec. Pap.* **82,** 31.

CURTIS, C. D. (1964) Application of the crystal field theory to the inclusion of trace transition elements in minerals during magmatic differentiation. *Geochim. Cosmochim. Acta* **28,** 389–403.

DVIR, M., AND W. LOW (1960) Paramagnetic resonance and optical spectrum of iron in beryl. *Phys. Rev.* **119,** 1587–1591.

HOLMES, OWEN G., AND DONALD S. MCCLURE (1957) Optical spectra of hydrated ions of the transition metals. *Jour. Chem. Phys.* **26,** 1686–1694.

LORD, R. C., R. S. MCDONALD AND FOIL A. MILLER (1952) Notes on the practice of infrared spectroscopy. *Jour. Opt. Soc. Am.* **42,** 149–159.

LOW, W. AND M. WEGER (1960) Paramagnetic resonance and optical spectra of divalent iron in cubic fields, I. Theory, II. Experimental results. *Phys. Rev.* **118,** 1119–1136.

MCCLURE, DONALD S. (1959) Electronic spectra of molecules and ions in crystals, II. Spectra of ions in crystals. In, *Solid State Physics*, Academic Press, New York, **9,** 399–525.

——— (1962) Optical spectra of transition metal ions in corundum. *Jour. Chem. Phys.* **36,** 2757–2779.

SLACK, GLEN A. (1964) $FeAl_2O_4$-$MgAl_2O_4$: Growth and some thermal, optical and magnetic properties of mixed single crystals. *Phys. Rev.* **134,** A1268–A1280.

TANABE, Y., AND S. SUGANO (1954) On the absorption spectra of complex ions. *Jour. Phys. Soc. Japan* **9,** 753–779.

ZUSSMAN, J. (1955) The crystal structure of an actinolite. *Acta Cryst.* **8,** 301–308.

Manuscript received, October 25, 1966; accepted for publication, December 25, 1966.